Large eddy simulations of flame extinction in a turbulent line burner

G. Maragkos, B. Merci

Department of Flow, Heat and Combustion Mechanics, Ghent University, St. Pietersnieuwstraat 41, B-9000 Ghent, Belgium

Abstract

Large eddy simulations of flame extinction with N_2 as extinguishing agent are performed focusing on combustion modelling with infinitely fast chemistry. EDM and EDC combustion models, an enthalpy-based flame extinction model based on a locally variable critical flame temperature and WSGGM for radiation are employed in order to predict flame extinction in a turbulent CH_4 line burner. The numerical predictions of mean thermocouple temperatures, combustion efficiencies and radiative fractions with different grid sizes are compared to the experiments by White et al. (2015).

Overall, the results from the numerical simulations agree well qualitatively and, to some extent, quantitatively with the experimental data when small grid sizes are employed. The examined centerline and radial profiles at two axial locations of the mean temperatures are reasonably well predicted. The decrease in the combustion efficiencies as the extinction limit is approached is reproduced by the numerical simulations. The decreasing trend in the radiative fractions as the oxidizer stream is diluted with N_2 is also captured by the simulations using a WSGGM model for radiation. Nevertheless, the influence of the combustion model is shown to be substantial towards predicting flame extinction due to differences in the predicted flame temperatures. Equally important is the influence of the simple re-ignition model based on a constant re-ignition temperature.

Keywords: flame extinction, LES, EDM, EDC, WSGGM, FireFOAM

1. Introduction

Flame extinction is a complex physical process which has received a lot of attention from the scientific community in the past and is inherently important when it comes to fire safety engineering since it deals with the protection of material property (i.e., industrial and/or residential) but also with the life safety of the public. The use of Computational Fluid Dynamics (CFD) in this area of research is crucial and its advantages are multifold. The use of CFD can be used towards evaluating the performance of current fire detection systems, the design and testing of new ones but also the virtual simulation of a wide range of hypothetical fire scenarios that in reality would either be too expensive to conduct, too complex to analyze by analytical solutions and/or zone models.

Flame extinction can be broadly described as the reduction of the chemical reaction rate below a critical value such that self-sustained combustion cannot occur. In general, three different mechanisms of extinction can be defined [1]: aerodynamic quenching (i.e., reduction of the flame residence times through flow perturbations), thermal quenching (i.e., radiative heat losses and/or water droplet evaporation) and quenching by dilution (dilution of the fuel and/or the oxidizer stream). Given the type of scenarios usually involved in fire applications, thermal quenching and quenching due to dilution are expected to be the predominant mechanisms for flame extinction since most flames are typically at low strain rates. Nevertheless, if scenarios would involve fires at high strain rates (e.g., presence of water sprays) then aerodynamic quenching will be important as well.

Flame extinction will occur in under-ventilated fires if the oxygen levels within the compartment fall below a critical value. Numerical modelling of such scenarios (i.e., prediction of carbon monoxide and/or minor chemical species) would involve the consideration of finite rate chemistry which is often prohibitive for fire simulations due to the wide range of time and length scales involved. The use of infinitely fast chemistry, which is widely used for fire simulations, poses additional modelling challenges when it comes to predicting flame extinction and re-ignition. CFD models should, in practice, be applicable and produce reliable/accurate predictions for a wide range of conditions/scenarios if they are to be used for practical applications of fire safety engineering. It is clear that validation of CFD codes in a wide range of fire plumes test cases (i.e., different sizes and fuels) is a prerequisite before any attempt is made to model flame extinction. Even though

such efforts have already been made and CFD codes are continuously being validated (e.g., https://github.com/firemodels/fds) discrepancies/differences in the predictive capabilities between different CFD codes are still present (https://github.com/MaCFP/) and could perhaps be attributed to the simplistic approaches often employed in fire modelling (i.e., related to turbulence, combustion, radiation, convective heat transfer, etc.). With all of this in mind in is obvious that any attempt in modelling flame extinction and re-ignition using infinitely fast chemistry is directly linked and dependent on all of the above-mentioned aspects.

Currently, fire-related CFD codes mainly rely on the concept of either a critical flame temperature [2, 3, 4] or a critical Damköhler number [5, 6, 7, 8, 9, 10] to model flame extinction. The former is a simple approach which is incorporated in the CFD code Fire Dynamics Simulator (FDS) (https://pages.nist.gov/fds-smv/) and is widely used in the fire community. Nevertheless, even though this approach has been demonstrated to work well for vitiated flames at low strain rates it cannot accurately predict flame extinction in scenarios involving high strain rates (e.g., scenarios involving aerodynamic quenching). The latter approach, which accounts for the effect of the chemical time scales is considered to be better suited for such scenarios. Recently, the reactive volume fraction approach has also been proposed [11] which considers an energy balance in eddies where fuel, oxidizer and combustion products are mixed together. This approach is currently available in the CFD code FireFOAM (https://github.com/fireFoam-dev) developed by FM Global.

The work presented here aims to continue the authors' previous work [12, 13] towards predictive fire modelling. The main objective of the paper is the application of the previously implemented modelling approaches related to turbulence, combustion and radiation modelling along with the use of an enthalpy-based extinction model using a variable critical flame temperature and their evaluation when it comes to predicting flame extinction with infinitely fast chemistry. Special focus is given on the influence of combustion modelling and the parameters involved in the flame extinction/re-ignition models. It is worth emphasizing that in the current work the radiative fractions are not prescribed a priori, based on known experimental data, rather they are predicted. For this purpose, Large Eddy Simulations (LES) of a turbulent CH_4 line burner with N_2 as extinguish agent are presented and the results are compared to the experiments by White et al. [14]. It is worth mentioning that experiments with C_3H_8 as fuel are also available. The choice to

simulate an experimental database which involves a non-sooty fuel was intentional in order to avoid, at this moment at least, the need for soot modelling. The chosen experiments are very relevant for the fire research community since they are one of the target test cases of the newly established Measurement and Computation of Fire Phenomena (MaCFP) workshop [36], focusing on advancing predictive fire modelling. The present target case is deemed suitable for evaluation/validation purposes of CFD codes with regards to flame extinction. The current work builds on the knowledge obtained from previous numerical works on the same test case [4, 15, 8] and aims to contribute to the modelling efforts of the fire community towards predicting flame extinction with infinitely fast chemistry within the LES context.

2. Modelling

The CFD code FireFOAM (https://github.com/fireFoam-dev), developed by FM Global, is employed here. The code uses a fully compressible flow formulation and solves the Navier-Stokes equations, along with transport equations for species mass fractions and sensible enthalpy, using Favre-filtered quantities, assuming a unity Lewis number. The models employed to model turbulence, combustion and radiation have been previously presented in [12, 13, 16] so only a brief overview is outlined here. It is worth noting that in the experiments considered here, a small laminar region has been reported just above the fire source (y < 5 cm) [6]. Nevertheless, given the fact that this region is relatively small compared to the experimentally reported flame height (i.e., about 50 cm), no special treatment regarding molecular diffusion modelling was deemed necessary.

The dynamic Smagorinsky model [17] is used to model turbulence, calculating the sub-grid scale viscosity as:

$$\mu_{sgs} = \overline{\rho}(c_s\Delta)^2|\widetilde{S}| \tag{1}$$

with the sub-grid kinetic energy is estimated as:

$$k_{sgs} = c_I\Delta^2|\widetilde{S}|^2 \tag{2}$$

where $\widetilde{S}$ is the resolved strain rate and the coefficients c_s and c_I are determined based on a dynamic procedure. Additionally, a variable Prandtl number formulation [18] is employed.

The sub-grid scale dissipation rate is modelled as:

$$\epsilon_{sgs} = \frac{c_\epsilon k_{sgs}^{3/2}}{\Delta} \tag{3}$$

where $c_\epsilon = 1.0$ [13] is a model constant.

Combustion is considered to be infinitely fast employing a one-step, irreversible chemical reaction for CH_4. For modelling turbulence-chemistry interaction two different models are considered, the Eddy Dissipation Concept (EDC) [19] and the Eddy Dissipation Model (EDM) [20]. Both models are typically employed in simulations of fire scenarios, hence, it is of great interest to evaluate their performance with respect to flame extinction. Within EDC, the fuel reaction rate is calculated as:

$$\overline{\dot{\omega}_F'''} = \overline{\rho} \frac{\gamma^2 \chi}{\tau_{EDC}(1 - \gamma^3 \chi)} min\left(\widetilde{Y}_F, \frac{\widetilde{Y}_{O_2}}{s}\right) \tag{4}$$

where $\overline{\rho}$ is the filtered density, γ is the size of the fine structures, τ_{EDC} is the EDC mixing time scale, χ is the reactive part of the fine structures, s is the oxygen-fuel mass stoichiometric ratio while $\widetilde{Y}_F$ and $\widetilde{Y}_{O_2}$ are the filtered mass fractions of fuel and oxygen, respectively.

The size of the fine structures can be expressed as:

$$\gamma = C_\gamma \left(\frac{\nu \epsilon_{sgs}}{k_{sgs}^2}\right)^{1/4} \tag{5}$$

with $\gamma <= 1$ and $C_\gamma = 2.1377$ the standard EDC model parameter.

For infinitely fast chemistry, χ is calculated as [21]:

$$\chi = \begin{cases} \frac{s\widetilde{Y}_{ref} + Y_{O_2}^0}{Y_{O_2}^0}, & \text{if } \widetilde{Y}_{ref} < 0 \\ \frac{Y_F^0 - \widetilde{Y}_{ref}}{Y_F^0}, & \text{if } \widetilde{Y}_{ref} \geq 0 \end{cases} \tag{6}$$

where Y_F^0 is the initial fuel mass fraction in the fuel stream, $Y_{O_2}^0$ is the initial oxygen mass fraction in the oxidizer stream and $\widetilde{Y}_{ref} = \widetilde{Y}_F - \widetilde{Y}_{O_2}/s$. In cases where finite rate chemistry is employed, it has been reported that the reacting part of the fine structures can be taken as unity [22] without any significant loss in accuracy. Nevertheless, this simplification may not be valid in cases where non-stoichiometric conditions with low turbulence Reynolds number

and incomplete reactions are present [34]. It is worth noting that application of a more sophisticated model, used by several authors in the past (e.g., [34]) for calculating the reacting part of the fine structures, did not reveal any significant influence in the predictions.

The estimation of the mixing time scale, τ_{EDC}, is modified compared to the original formulation of the model as:

$$\tau_{EDC} = \min(\tau_{turb}, \tau_{lam}); \tag{7}$$

which effectively considers mixing under turbulent and laminar conditions. The turbulent time scale is based on the original energy cascade model by Ertesvåg and Magnussen [23], taken as the Kolmogorov time scale:

$$\tau_{turb} = C_\tau \left(\frac{\nu}{\epsilon_{sgs}}\right)^{0.5} \tag{8}$$

where $C_\tau = 0.4082$ is the standard EDC model parameter while the laminar time scale is estimated as:

$$\tau_{lam} = \frac{\Delta^2}{C_{diff}\nu} \tag{9}$$

where $C_{diff} = 4$ [13] is a model constant.

Within EDM, the fuel reaction rate is calculated as:

$$\overline{\dot{\omega}_F'''} = \bar{\rho}\frac{min(\widetilde{Y}_F, \widetilde{Y}_{O_2}/s)}{\tau_{EDM}} \tag{10}$$

with the mixing time scale, τ_{EDM}, calculated as:

$$\tau_{EDM} = min\left(\frac{k_{sgs}}{C_{EDM}\epsilon_{sgs}}, \frac{\Delta^2}{C_{diff}\alpha}\right) \tag{11}$$

which essentially considers an estimate of the fuel-air mixing, under turbulent and laminar flow conditions, respectively. The model constants are assigned the values $C_{EDM} = 4$, $C_{diff} = 4$ [12].

It is important to note that there is a significant difference in the mixing time scales involved in the two combustion models employed in the current study. The use of the dynamic model for calculating the sub-grid scale kinetic energy (Eq. (2)) and the choice of the closure model for the sub-grid scale dissipation rate (Eq. (3)) results in a grid-independent mixing time scale in

the case of EDM. This is not the case for EDC since the use of the Kolmogorov time scale within the LES context results in τ_{EDC} being dependent on Δ. Ideally, numerical models should rely on physical parameters and not be explicitly grid dependent (which is rather artificial). Important can also be the influence of turbulence modelling, particularly the calculation of the sub-grid scale kinetic energy, k_{sgs}, in the numerical simulations. Even though not explored within the context of the present work, obviously this aspect can also have a direct influence on the reaction rates predicted by the combustion model.

The radiation modelling employed in this study, considers the dependency of the radiative intensity on both the spatial location and the angular direction and is obtained by solving the radiative transfer equation (RTE) by the finite volume discrete ordinates model (fvDOM). The absorption/emission is modelled through the weighted-sum-of-gray-gases model (WSGGM), a model which lies between the over-simplified gray gas model and the complete model which considers particular absorption bands. Within WSGGM, the total emissivity and absorptivity (assuming $\alpha = \epsilon$) of a gas mixture is calculated as the sum of fictitious gray gases (i.e., CO_2 and H_2O) weighted with a temperature dependent weighting factor as:

$$\widetilde{\epsilon} = \sum_{i=0}^{I} \widetilde{a}_{\epsilon,i}(T)\big(1 - e^{-\kappa_i p L}\big) \tag{12}$$

where $a_{\epsilon,i}$ is the emissivity weight factor of the i fictitious gray gas, κ_i is the absorption coefficient of the i gray gas, p is the sum of the partial pressures of all absorbing gases and L is the path length, calculated as $L = 3.6V/A$. The volume, V, is calculated by summing all the cell volumes where reaction takes place. Assuming a rectangular shape (due to the burner geometry), then the corresponding surface area, A, is calculated. This dynamic approach of calculating the beam length was chosen in order to incorporate, to a certain extent, the reduction in the size of the absorption medium when a fire tends towards the extinction limit.

The temperature dependence of $a_{\epsilon,i}$ is calculated as:

$$\widetilde{a}_{\epsilon,i} = \sum_{i=0}^{J} b_{\epsilon,i,j}\widetilde{T}^{j-1} \tag{13}$$

where $b_{\epsilon,i,j}$ are the emissivity gas temperature polynomial coefficients. The coefficients $b_{\epsilon,i,j}$ and κ_i are taken from [24]. The total absorptivity is then

7

calculated as:

$$\widetilde{a} = -\frac{ln(1 - \widetilde{\epsilon})}{L} \tag{14}$$

and the radiative heat fluxes are calculated as:

$$\nabla \cdot \overline{\dot{q}_r''} = \widetilde{a}(4\sigma\widetilde{T}^4 - \widetilde{G}) \tag{15}$$

where σ is the Stefan-Boltzmann constant and G is the total irradiance. Turbulence-chemistry interaction (TRI) is neglected at present. The current approach aims to accurately predict the radiative fractions in the numerical simulations, as opposed to prescribing them a priori. The experimental case considered here employs CH_4 as fuel which is only slightly sooty, hence, soot modelling has been neglected.

The modelling approach employed to account for local extinction considers an enthalpy balance based on the concept of a critical flame temperature. The criterion examines whether a reactant mixture within a computational cell will have enough energy to raise its temperature above a critical flame temperature to sustain combustion and is expressed as [3, 25]:

$$\hat{Y}_F(h_F(\widetilde{T}) + \Delta H_{c,F}) + \hat{Y}_O h_O(\widetilde{T}) + \hat{Y}_D h_D(\widetilde{T}) >$$
$$\hat{Y}_F h_F(T_{CFT}) + \hat{Y}_O h_O(T_{CFT}) + \hat{Y}_D h_D(T_{CFT}) \tag{16}$$

where $\hat{Y}$ are the mass fractions, h are the sensible enthalpies, the sub-scripts F, O and D denote the fuel, oxidizer (i.e., air) and diluents (i.e., inert gases or products of combustion) present in the reactant mixture, $\widetilde{T}$ is the (filtered) initial cell temperature, $\Delta H_{c,F}$ is the heat of combustion of the fuel and T_{CFT} is a critical flame temperature. The composition of the reactant mixture within a computational cell that can react is calculated based on the composition of the species present in that cell as $\hat{Y}_F = min(\widetilde{Y}_F, \widetilde{Y}_O/s)$, $\hat{Y}_O = s\hat{Y}_F$, $\hat{Y}_D = (\hat{Y}_O/\widetilde{Y}_O)(\widetilde{Y}_F - \hat{Y}_F + \widetilde{Y}_D)$ where $\widetilde{Y}_F, \widetilde{Y}_O, \widetilde{Y}_D$ are the (filtered) mass fractions of fuel, oxidizer and diluents in the computational cell and s is the oxidizer to fuel mass ratio. The enthalpy balance is based on the initial composition of the reactant mixture before any combustion is computed (i.e., after scalar transport but before any reaction). If the inequality is false then reaction within a computational cell is inhibited for the current time step. Based on the formulation of the model, any excess fuel within a cell acts as a diluent while any excess air does not. In general, the model is applicable to scenarios involving thermal quenching and quenching by dilution, since both mechanisms can be accounted for in the enthalpy balance.
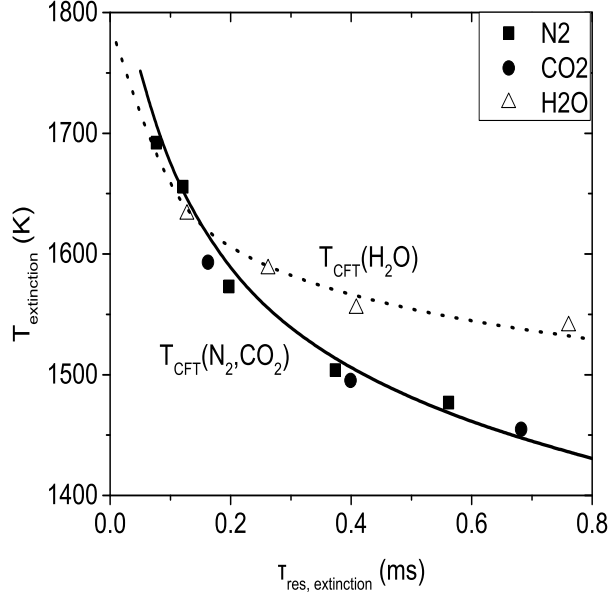
Figure 1: Extinction temperature vs residence time at extinction. Data: Perfectly Stirred Reactor (PSR) simulation data taken from [15], Lines: power law-fitted critical flame temperatures (T_{CFT}).

For the evaluation of the flame extinction criterion, a critical flame temperature, T_{CFT}, is needed. A fixed value of 1780 K [26] is suggested by the CFD code Fire Dynamics Simulator (FDS) for methane (i.e. the temperature at the limiting oxygen index). A sensitivity study with values between $T_{CFT} = 1500-1700$ K in [4] revealed some sensitivity in the numerical predictions when simulating the same test case. A different approach is employed here which allows the critical flame temperature, T_{CFT}, to vary depending on the local composition and residence time in every computational cell. The extinction temperatures as a function of the residence times, τ, are taken the from Perfectly Stirred Reactor simulations for different diluent agents (N_2, CO_2, H_2O) with varying concentrations reported in [15] (shown in Figure 1).

The critical flame temperatures based on the local inert (N_2, CO_2) and non-inert diluents (H_2O) are given by a power law in the the following form:

$$T_{CFT, \, (N_2, CO_2)} = 1407.4\tau^{-0.073} \tag{17}$$

$$T_{CFT, \, (H_2O)} = 1517.8\tau^{-0.034} \tag{18}$$

9

where as τ the equivalent time scale of each combustion model (i.e, τ_{EDM} or τ_{EDC}) is used.

The local critical flame temperature in every cell is then calculated as a mass-weighted average of these two critical flame temperature as:

$$T_{CFT} = (Y_{N_2} + Y_{CO_2}) \times T_{CFT, \; (N_2,CO_2)} + Y_{H_2O} \times T_{CFT, \; (H_2O)} \qquad (19)$$

The resulting critical flame temperatures are bounded between 1480 K and 1780 K, values which are common minimum and maximum limits for most hydrocarbon fuels. In general, different approaches can be employed for determining T_{CFT} (e.g., from PSR simulations, opposed flow calculations with detailed chemistry, experiments) for different fuels when data are not available. Alternatively to what is employed in this study, T_{CFT} values as a function of strain rate from opposed flow calculations with detailed chemistry [27] can also be considered, bringing this way some sub-grid scale effects in the flame extinction modelling.

Flame re-ignition is also an important aspect when it comes to modelling flame extinction with infinitely fast chemistry. At any point in space and time, any unburned fuel in the computational domain can mix with the oxidizer and react regardless of the temperature of the mixture. This behavior is not realistic and can cause erroneous phenomena of re-ignition further downstream from the fire source where they should not be present [4]. For this reason, an ignition temperature, T_{ign}, is specified in the numerical simulations which controls when any re-ignition phenomena can occur. This criterion essentially only allows any unburned fuel to react with the oxidizer if the temperature in the computational cell is above the specified T_{ign} value (and the enthalpy balance in Eq. (16) is satisfied) expressed as:

$$\widetilde{T} > T_{ign} \qquad (20)$$

Nevertheless, this approach cannot be globally applied within the entire computational domain without affecting the primary ignition and combustion process. Following the work performed by White et al. [4], a small pilot flame area just above the fuel inlet, 25 mm in height, is specified in which combustion is allowed to take place without allowing for any flame extinction or re-ignition to occur (i.e., both phenomena essentially cannot occur there). Inside this region it is $T_{ign} = 0$ K. For the region outside the pilot flame area, $T_{ign} = 1100$ K is used, estimated from extrapolated values of ignition temperatures of methane combustion at low strain rates, typically found in

10

fires, based on [28]. This value is also close to the range of re-ignition temperatures suggested in [6] for the same test case. It is worth noting that this value is above the auto-ignition temperature of methane (i.e., 910 K for pure air at ambient temperature and atmospheric pressure). The use of this value is motivated by the fact that any re-ignition phenomena will occur for a lean methane mixture, diluted by hot air and combustion products, which will raise the ignition temperature of the mixture above the auto-ignition temperature of methane. Focusing on typical fire scenarios which involve relatively low turbulent Reynolds numbers, the main mechanisms for flame re-ignition are mainly due to premixed auto-ignition (controlled by chemistry) and non-premixed auto-ignition (controlled by mixing and chemistry). Both of these mechanisms require a temperature of approximately 1000K [29]. The selected re-ignition temperature in the present study is close to the above-mentioned value. Nevertheless, a more advanced re-ignition modelling approach, that is not based on a user input parameter, is worth considering in future numerical simulations. A possible approach could be the use of a re-ignition temperature as a function of strain rate for different methane dilution ratios based on [28] at an additional computational cost and added modelling uncertainty.

3. Experimental configuration

The turbulent line burner experiments performed by White et al. [14] are considered in this study which are one of the target cases of the newly established Measurement and Computation of Fire Phenomena (MaCFP) workshop [36]. The configuration, shown in Figure 2, consists of a CH_4 diffusion flame with a controlled co-flowing oxidizer of air. Fuel is issued at a mass flow rate of 1 g/s, corresponding to a total heat release rate of 50 kW for an unsuppressed flame, while the co-flowing oxidizer is issued at a mass flow rate of 85 g/s. A wall consisting of ceramic fiberboard separates the fuel port from the oxidizer stream. In the suppressed flame configurations, N_2 is used as an extinguishing agent. In these cases the mass flow rate of the air remained constant while nitrogen was added in the co-flow essentially varying the oxygen mole fraction from 21% to 11% in order to suppress the flames. Given the fact that the chosen experimental test case is well documented in the literature only a brief description is included here. More details regarding the experimental setup and the diagnostics used for the experimental measurements can be found in [4, 14] while the experimental
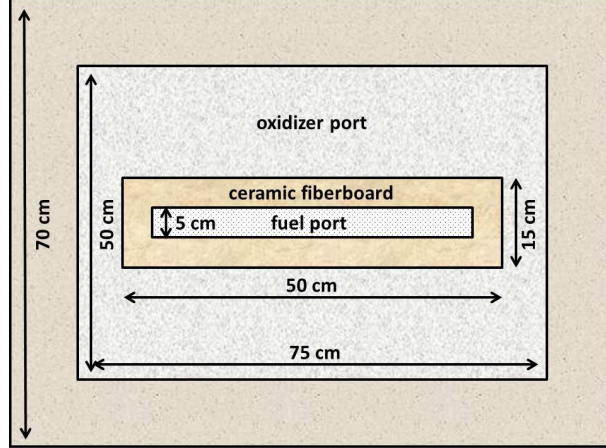
data are available through https://github.com/MaCFP/.

Figure 2: Top view of the fuel and co-flow outlets of the line burner.

4. Numerical setup

A computational domain of 1.6 m x 2 m x 1 m is used in the simulations shown in Figure 3. The base mesh consists of 25 mm cells stretched towards the top boundary (ratio of grid size heights at the top and bottom boundaries is 1.5). A refinement strategy is then employed in order to have a good grid resolution up to the experimentally reported flame height (i.e., 50 cm). A box having dimension of 0.8 m x 0.8 m x 0.6 m refines the mesh to 12.5 mm while a second box of dimensions 0.6 m x 0.6 m x 0.4 m refines the mesh to 6.25 mm. The total number of cells is then approximately 886000. Previous numerical studies [4, 6, 30] on the same test case have indicated that cell sizes in the order of 5 mm are needed to accurately simulate this scenario. The chosen grid size in our study is on the same order of magnitude.

The methane mass flow rate is set to 1 g/s (50 kW), accounting for both convective and diffusive mass fluxes, while the co-flowing oxidizer is provided at 85 g/s, according to the experiments. The ambient temperature and pressure are 293 K and 101325 Pa, respectively. The ceramic fiberboard plate (separating the fuel inlet and co-flow air at y=0) is treated as a no-slip isothermal wall. For the simulations involving flame extinction, the oxygen mass fraction in the oxidizer port is initially maintained at $Y_{O_2} = 0.233$ for 4 s and is subsequently decreased by 0.005/s (followed by equivalent increase
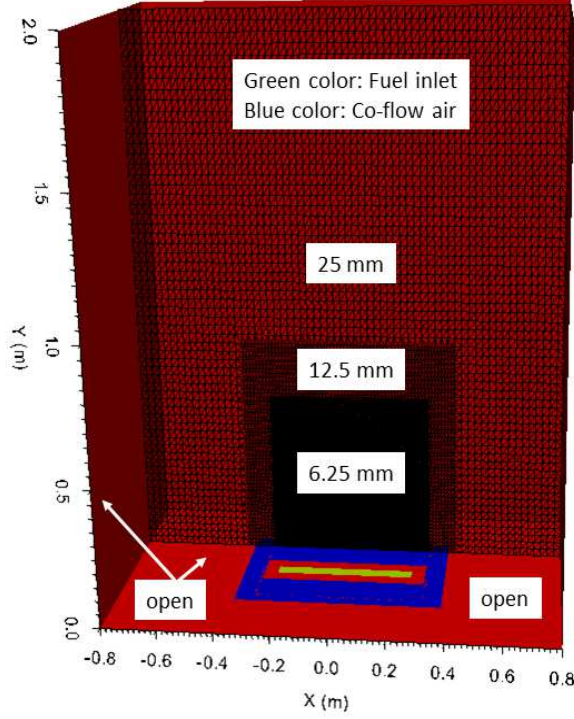
Figure 3: Geometry and computational mesh used in the numerical simulations.

in Y_{N_2}). Regarding radiation modelling, 48 solid angles were used for angular discretization. This number has been reported to be sufficient for radiative heat transfer inside the structure of fire plumes [13, 31]. Nevertheless, for accurate predictions of the experimental radiative heat fluxes in this case approximately 300 solid angles would have been needed [6, 30]. This was not the case in the present study. All numerical simulations were set to run for 40 sec with a varying time step, limited by a maximum Courant number of 0.9. The equations are advanced in time using a first order Euler scheme. The convective terms are discretized with a second order central difference scheme while for scalar transport a second order TVD scheme using a Sweby limiter is applied. A PIMPLE algorithm is used for the pressure-velocity coupling with a Rhie-Chow interpolation to avoid odd-even decoupling. The bottom plane (at $y = 0 \ m$), outside the co-flowing air, along with the sides of the computational domain were set as open, allowing air to be entrained into the domain. A mixed boundary condition is assigned for velocity at these

13

boundaries, setting zero gradient for any outward flow and calculating the inlet velocity from pressure while a Dirichlet boundary condition is assigned for pressure which fixes total pressure, and when velocity changes, the pressure is adjusted accordingly. At the outlet, a Neumann (i.e., zero gradient) boundary condition is assigned for all variables with no reverse flow allowed in order to avoid numerical instabilities.

5. Results

5.1. LES resolution

As a first step, an evaluation of the accuracy of the LES simulations is presented in Figure 4. A quantitative analysis on the chosen grid is performed by comparing the turbulence resolution, k_{res}/k_{total}, and the ratio of sub-grid scale to molecular viscosities, μ_{sgs}/μ in the numerical simulations. Results on the centerline are presented with the EDM combustion model only for illustrative purposes even though very similar results were obtained with EDC as well. The resolved kinetic energy is calculated as $k_{res} = \frac{1}{2}\big(u_{rms}^2 + v_{rms}^2 + w_{rms}^2\big)$ where u, v and w are the three velocity components, k_{sgs} is obtained from the turbulence model (Eq. (2)) while $k_{total} = k_{res} + k_{sgs}$.

As expected, the turbulence resolution is lower close to the fuel inlet, due to combustion and buoyancy generated turbulence in this region, and gradually increases as we move further downstream. The coarser grid cases obviously result in lower turbulence resolutions close to the fire source. Nevertheless, the turbulence resolution with the finest grid employed (i.e., 6.25 mm) is relatively high and remains significantly over 80 % in accordance with Pope's criterion [37]. Care should be taken, however, when evaluating LES grids with this criterion since the turbulent resolution can be affected by the choice of the numerical schemes employed (i.e. dissipative schemes will over-estimate the simulation quality [38]). The actual values of the turbulent resolution in the numerical simulations are likely to be lower for the reason mentioned above. The maximum values for the sub-grid scale to molecular viscosity ratio for the finest grid size are close to unity in the main region of interest (i.e., $y < 0.6$ m which covers the experimentally reported flame height of 50 cm). This implies that turbulence modelling, even though still important, is comparable in magnitude to molecular transport. However, we should also have in mind that the dynamic procedure involved in the determinations of the Smagorinsky constant occasionally leads to negative values, particularly in laminar regions like the one reported experimentally

14

above the line burner. This implies that in these regions the sub-grid scale viscosity is zero since c_s is clipped to also zero. Clearly the jumps observed in the profiles for all cases relate to the refinement grid strategy employed in the study which occur at $y = 0.6$ m and $y = 0.8$ m. For completeness, it is reported that similar comments could be made for the radial profiles of both the turbulence resolution and viscosity ratios which were examined at different heights above the burner (results not shown here). The results presented above indicate that the finest grid employed in the present study (i.e., 6.25 mm) is sufficiently small to capture most of the flow dynamics of the turbulent line burner.
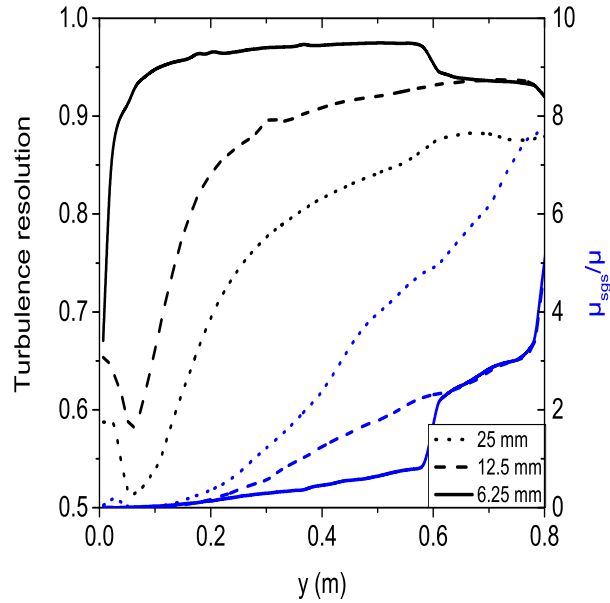
Figure 4: Turbulence resolution (left) and ratio of sub-grid scale to molecular viscosities (right) on the centerline as a function of grid size with the EDM combustion model.

5.2. Average results

The average results presented in this section involve cases (i.e., $X_{O_2} = 0.21$ or $X_{O_2} = 0.18$) where the oxygen mole fraction in the co-flow was not close to the limiting oxygen concentration for extinction (i.e., $X_{O_2, \ ext} \approx 0.12$). In these cases, the extinction model was not employed as the experimentally measured combustion efficiency was about 99%. Another reason

is the influence of the extinction/re-ignition model on the predicted combustion efficiencies, when coarse grids are employed, which would inhibit any meaningful comparisons between simulations and experiments (see next section). The reported temperature results are thermocouple temperatures obtained from a simple thermal balance for the thermocouple bead (treated as a thermally-thin device) as described in [32].
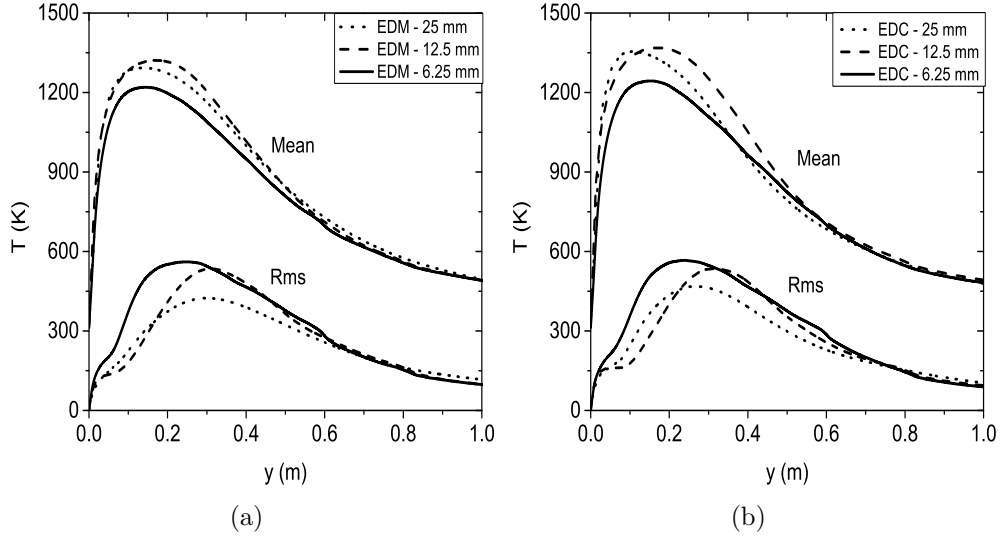

Figure 5: Predicted thermocouple temperatures on the centerline with (a) EDM and (b) EDC for $X_{O_2} = 0.21$ in the oxidizer stream.

The centerline mean and rms temperatures for different mesh sizes are first presented in Figure 5 for a test case with $X_{O_2} = 0.21$ in the oxidizer stream. Maximum flame temperatures of approximately 1245 K and 1220 K are predicted with the finest grid size (i.e., 6.25 mm) with EDC and EDM, respectively, with an increase in the rms temperatures as the grid size decreases. The lower maximum flame temperatures obtained with the finer grids, as opposed to the coarser grid cases, are attributed to a combined effect of turbulence, combustion and radiation. Even though the integrated reaction rates for all cases were the same (i.e., 1 g/s), the reaction rates close to the fuel source decrease significantly and shift slightly downstream with decreasing grid size. Generally, slightly higher reaction rates are predicted on the centerline with the EDC as opposed to the EDM (Figure 6) which is a direct consequence of the differences in the calculation of the mixing times scales between the models (i.e., smaller mixing times scales in the case of

16

EDC). This aspect combined with the fact that the grid size of 25 mm is relatively coarse which dissipates the flow and produces more laminar-like flame structures (i.e. only two cells across the width of the burner) results in the fuel to react instantly and produce high reaction rates just above the burner. As the grid size is refined, fuel rich conditions above the burner along with the fact that the fire plume is now more turbulent reduce the maximum reaction rate value and shift its peak further downstream. The centerline temperatures obtained with both models are close to the experimental measurements (data not shown here but reported in [39]) only on the finer grid employed for the reasons explained above. The predicted radiative fractions in the case of EDC remained relatively constant with grid size, while an increase was observed for the case of EDM. More specifically, the predicted radiative fractions for EDC were 0.214, 0.219, 0.215 while for EDM they were 0.190, 0.202, 0.213 for the 25, 12.5 and 6.25 mm cases, respectively, while the experimental value was about 0.23. For completeness, the predicted radiative fractions for the case with $X_{O_2} = 0.18$ in the oxidizer stream are also reported. In this case, the predicted χ_r values for EDC were 0.194, 0.197, 0.193 while for EDM they were 0.171, 0.180, 0.189 for the 25, 12.5 and 6.25 mm cases, respectively, while the experimental value was about 0.195. The higher radiative fractions predicted with EDC, compared to EDM, are in fact not suprising given the fact that higher temperatures are predicted as well. Overall, similar trends are found from the application of both the EDM and the EDC models, namely over-predicted flame temperatures when coarse grids are employed, similarly to some extent to what has been reported in [4] for the same test case. It is postulated that part of the reason of these discrepancies here could be related to turbulence modelling and the calculation of k_{sgs} more in specific that might need further investigation in the future.

The radial profiles of the mean temperatures with both combustion models at two different heights for a case with $X_{O2} = 0.18$ in the oxidizer stream are presented in Figures 7-8. As expected, lower maximum centerline flame temperatures and wider profiles are observed with increasing distance from the burner. Overall, the numerical predictions with the finest grid size employed (i.e. 6.25 mm) are able to reproduce quite reasonably both the flame width and the maximum flame temperatures at these two heights. Even though somewhat counter-intuitive, over-predictions in the maximum flame temperatures are observed for the coarser grids for the reasons described above.

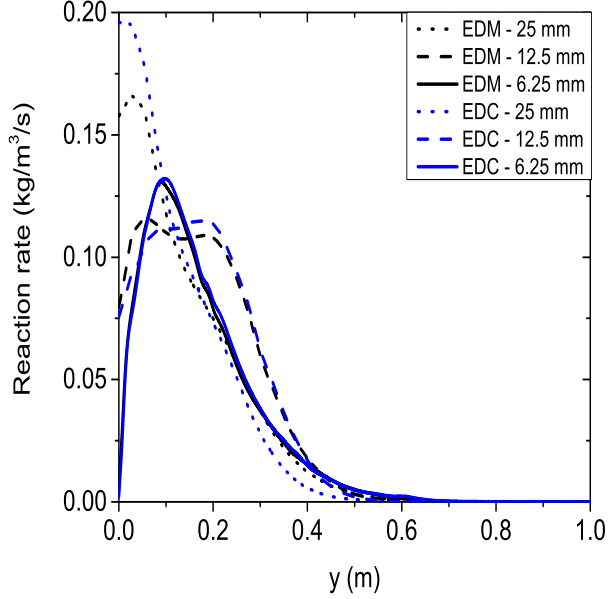The results with the EDC combustion model reveal an over-prediction

Figure 6: Predicted reaction rates on the centerline with EDM and EDC for $X_{O_2} = 0.21$ in the oxidizer stream.

of the resulting temperatures, when compared to the experimental ones but also with the EDM results, over all the grid sizes examined. Generally, similar findings have been reported in the past from the use of EDC for various applications (e.g., [33, 34]). Additionally, it is well established that the EDC combustion model is not valid in regions where the flow is laminar since the model has been derived for turbulent flows. This is the case for most fire scenarios since they involve relatively low Re_t numbers and transition to turbulence occurs only when moving away from the fire source. Several approaches have been employed in literature to remedy these deficiencies of the model ranging from, e.g., adjusting the model coefficients, modifying the calculations of the residence times or using Arrhenius reactions when the flow conditions are laminar. All of the above-mentioned approaches were tested by the authors and it is worth reporting several findings. Modifying the model constants, either arbitrarily either through re-calibration based on another turbulence model, had a significant influence on the predicted temperatures, but unless a systematic evaluation of the modified constants is made on several test cases it would be difficult to make concrete suggestions. It is worth noting that, in the initial formulation of the EDC model, C_γ was

18
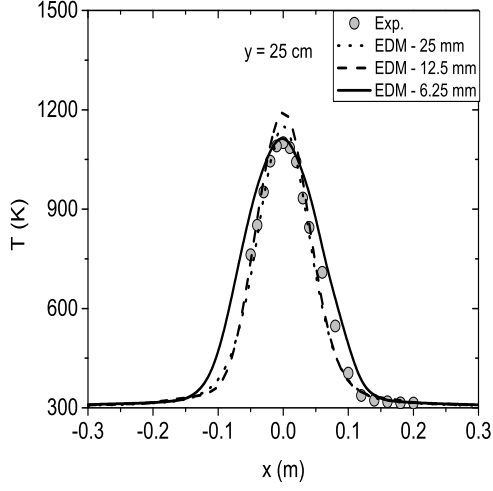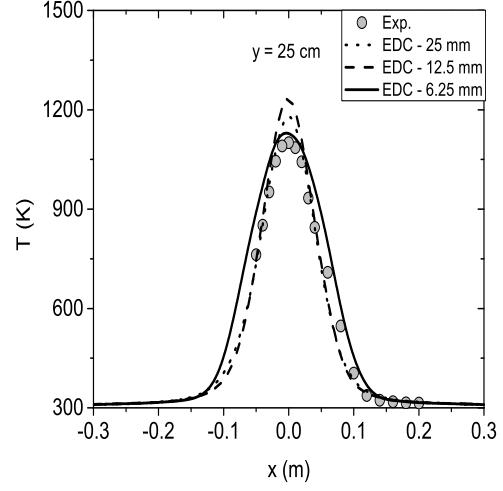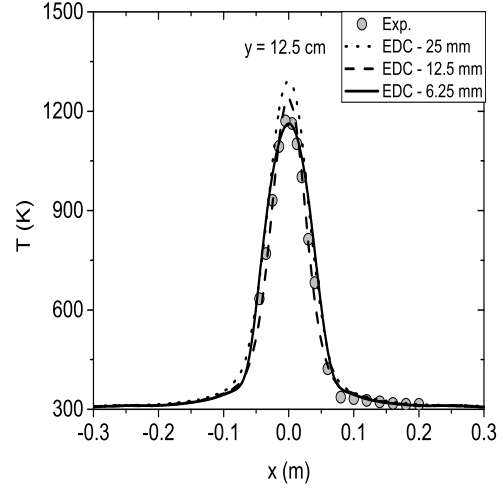
(a)
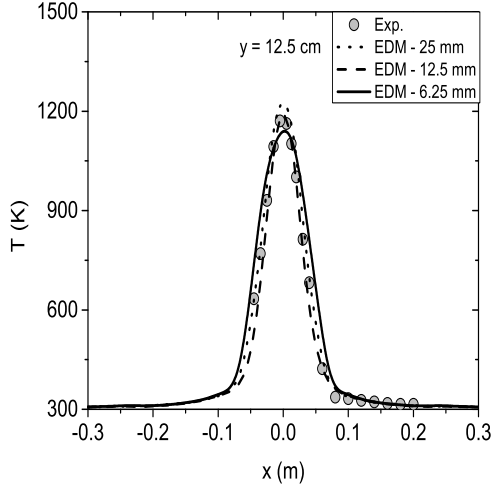
(b)

Figure 7: Radial profiles of thermocouple temperature with EDM at height (a) y=25 cm and (b) y=12.5 cm for $X_{O_2} = 0.18$ in the oxidizer stream.

(a)

(b)

Figure 8: Radial profiles of thermocouple temperature with EDC at height (a) y=25 cm and (b) y=12.5 cm for $X_{O_2} = 0.18$ in the oxidizer stream.

derived based on the k-ϵ model and C_τ was fitted based on various experimental data. The parameter C_γ can be re-calibrated based on the employed turbulence model at hand but a similar fitting of C_τ based on different experimental cases of fire plumes is perhaps worth exploring in the future. The use of dynamically determined coefficients is a possible option (also employed by the authors in the past [13]). However, it requires additional modelling and the need to define bound for the model constants. Equally influential was the use of modified residence times, either by considering, e.g., the integral time scale or the geometrical mean of the Kolmogorov and the integral time scale [35] (still having a grid dependency in this latter case). Reduction in the resulting flame temperatures was observed in both cases, however, this was occasionally also accompanied by lower heat release rates as well. An attempt to employ an Arrhenius reaction in regions where the flow was laminar was also made. Such an approach, however, strongly depends on the calculation of Re_t and also adds to the modelling uncertainty (i.e., requires choice of the Arrhenius constants for the reaction). In addition, the consideration of finite rate effects would potentially lead to inconsistencies with the flame extinction modelling approach employed.

5.3. Transient results

5.3.1. Combustion efficiency

The combustion efficiency from the numerical simulations is calculated as the ratio of the integrated heat release rate (HRR) in the computational domain over the HRR at the fuel source which is expressed as:

$$\eta_{comb} = \frac{\iiint_V \overline{\dot{\omega}_{h_s}'''} dV}{\dot{m}_{fuel} \Delta H_{comb}} \tag{21}$$

where $\overline{\dot{\omega}_{h_s}'''}$ the local volumetric heat release rate in every cell, $\dot{m}_{fuel}$ is the mass flow rate of fuel at the burner and ΔH_{comb} is the heat of combustion of the fuel. For the presentation of the combustion efficiency results below, a time-averaging window of 200 time steps (i.e., ≈ 1 s) has been used.

From the combustion efficiency results presented in Figure 9, it is interesting to note that the numerical predictions with the coarsest grid (i.e., 25 mm) are strongly affected by the extinction/re-ignition model and cannot accurately simulate the scenario in the case of EDM. As the grid size is refined to 12.5 mm this influence vanishes and the combustion efficiency remains around 1 in the initial stage when $X_{O2} > 0.18$ in the oxidizer stream.
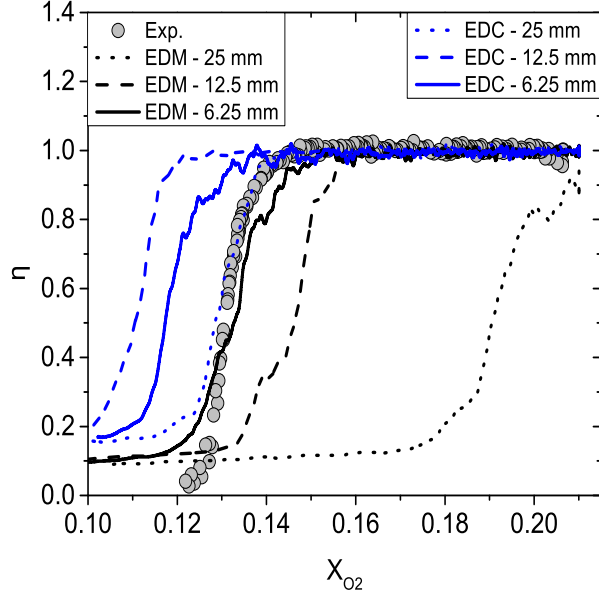
20

Figure 9: Predicted combustion efficiency with EDM and EDC as a function of grid size.

Generally, the predictions with both the 12.5 mm and 6.25 mm grid sizes follow approximately the experimental trends and differences are mainly visible when approaching the extinction limit. The predictions with the 6.25 mm grid are in better agreement with the experiments, when compared to the 12.5 mm grid case, and are able to reproduce the experimental trends towards flame extinction (i.e., when $X_{O2} \approx 0.12$ based on the experimental data). Vastly different are the results obtained with EDC with a 25 mm grid size. The previously presented higher temperatures obtained with the model on coarser grids do not affect the combustion efficicencies and in fact the simulations are able to predict flame extinction around the same times as the experiments. At finer grids, the predicted combustion efficiencies still remain close to the experiments in the initial stages (i.e., close to unity) but delay to predict flame extinction for the reason explained above. Within this context, it is worth noting that the use of a higher re-ignition temperature would result in flame extinction to occur earlier and perhaps better match the experimental data. Based on these results, it is clear that the choice of the combustion model can have a significant influence when trying to model flame extinction with infinitely fast chemistry. In addition, a relatively fine grid is also needed in the numerical simulations in order to accurately predict

21

flame extinction. It is important to note that cell sizes in the order of cm or less are typically required for accurate modelling of pool fires [36]. This can perhaps pose some limitations in cases where large-scale fire scenarios need to be simulated.

The evaluation of the enthalpy balance (Eq. (16)) which determines whether extinction will occur or not is obviously strongly dependent on the choice of the critical flame temperature, T_{CFT}, but also on the choice of re-ignition temperature, T_{ign}. Even though they are both user defined parameters, the choice of them can be justified based on experimental works found in literature (e.g., consider as T_{CFT} the temperature at the limiting oxygen index and the re-ignition temperature to be taken as the auto-ignition temperature of the fuel). In fact, such choices are already considered by default in FDS and are reasonably chosen parameters. Nevertheless, there will inevitably be an influence of the local strain rate and the fuel dilution in the choice of these values depending on the scenario examined. Ideally both T_{CFT} and T_{ign} should be space and time dependent and vary during the simulations accounting for the local properties of the flow. An obvious disadvantage is that perhaps no experimental data exist for a wide range of fuels and dilution conditions that could be used as a database for CFD codes. Numerical experiments can be conducted for such cases at an increased effort and computational cost by the user. It is important to note that the relative choice of the T_{CFT} and T_{ign} values can be important. For example, increasing the T_{CFT}/T_{ign} values will result in flame extinction occurring sooner (i.e., shift of the combustion efficiency curve to the right) while decreasing the T_{CFT}/T_{ign} values will result in flame extinction to occur later (i.e., shift of the combustion efficiency curve to the left). With this in mind, different choices for T_{CFT} and T_{ign} can lead to similar numerical predictions of flame extinction due to compensating effects.

In this case, the predicted critical flame temperatures just above the fuel inlet were close to 1480 K (i.e., the lower bound set for T_{CFT}) and occasionally reached close to the upper bound (i.e., 1780 K) in the flaming region. Looking at how we would expect T_{CFT} to vary as a function of the local strain rate, these findings are in line with the fact that laminar structures were reported experimentally above the fuel source. Such regions with laminar-like structures would involve relatively low strain rates (i.e., high residence times), hence, lower critical flame temperatures would be expected. On the other hand, regions involving higher strain rates (i.e., low residence times) would result in higher flame temperatures at extinction. The consideration

of a variable calculation for the critical flame temperature is certainly more realistic, as opposed to using a constant value, and to a certain extent it can incorporate the different physics involved in flame extinction scenarios. Different methods of calculating T_{CFT} is surely something worth investigating in the future. Currently, the extinction model employed in this study does not include any strain rate or sub-grid scale effects. In addition, the model might not perform well for cases involing water sprays unless the water droplets have been fully evaporated since this effect is not accounted for in the enthalpy criterion. These are definitely some important aspects for research and further improvement of the model in the future.

5.3.2. Radiative fractions

The radiative fractions from the numerical simulations are calculated as the ratio of the integrated radiative heat fluxes at all domain boundaries over the heat release rate inside the computational domain as:

$$\chi_r = \frac{\iint_S \overline{\dot{q}_r''} dS}{\iiint_V \overline{\dot{\omega}_{h_s}'''} dV} \tag{22}$$

where $\overline{\dot{q}_r''}$ denotes the radiative heat fluxes while S represents the surface area of the computational domain.

In general, similar observations like the ones previously made for the combustion efficiencies can be made by examining the predicted radiative fractions, χ_r, shown in Figure 10. The experimental trends of decreasing radiative fractions as the flame extinction limit is approached is reproduced by the numerical simulations with both combustion models (excluding the 25 mm grid size with EDM). Reasonably good predictions are obtained for the 6.25 mm cases with both EDM and EDC. A substantial difference in the predictions with the two combustion models is that increasing χ_r values with decreasing grid sizes are obtained with EDM while the radiative fractions in the case of EDC increase from 25 mm to 12.5 mm and then decrease in the 6.25 mm grid size. This is attributed to the differences in the predicted flame temperatures between the models, also previously seen in the average results in Figure 5. However, the extinction model has an influence on the heat being released due to radiation in the initial stages when $X_{O2} > 0.15$ in the co-flow. The predicted radiative fractions for two simulated cases ($X_{O2} = 0.18$ and $X_{O2} = 0.21$) with a grid size of 6.25 mm without the activation of the extinction model reveal higher χ_r values for both combustions models. There
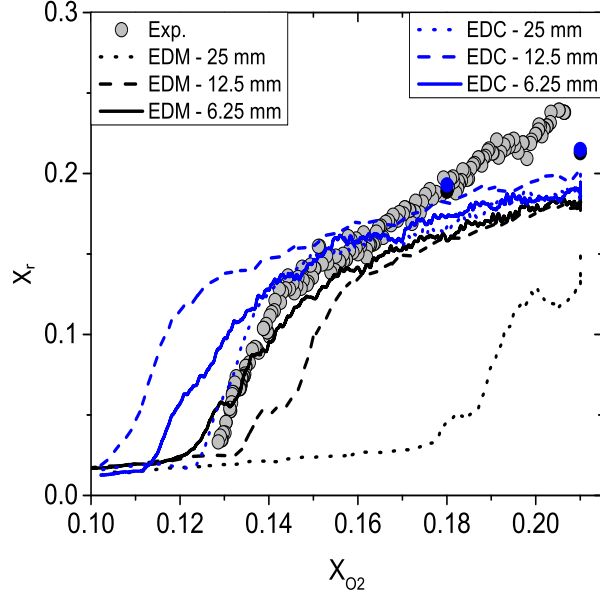
23

Figure 10: Predicted radiative fractions with EDM and EDC as a function of grid size. Black (EDM) and blue (EDC) circles denote the predicted χ_r values with no extinction model activated for a grid size of 6.25 mm.

is clearly a noticable influence of the extinction/re-ignition model towards reducing the resulting radiative emissions from the flames which is not a desirable aspect of the employed modelling approach. The differences are particularly bigger in the case of EDM as opposed to EDC. Nevertheless, there is still an under-prediction of the predicted radiative fraction when $X_{O2} = 0.21$ in the oxidizer stream with both models. The present simulations neglected any modelling of radiation-turbulence interactions (RTI). It has been supported in the past that consideration of TRI in turbulent flames can increase the radiative emissions through increased temperature fluctuations [40]. This aspect needs further investigation in the future. Numerical predictions recently reported by FDS in [25], employing two fast reactions, the first converting fuel to CO and soot, and the second converting CO and soot to CO2, have shown to predict quite well the radiative fractions when grid sizes smaller than 6.25 mm were employed. It needs further investigation whether the consideration of CO and soot in the radiation modelling could lead to an improvement in the present predictions as well.

It is worth noting that capturing this decrease in χ_r can be important

24

when trying to accurately predict flame extinction in any random fire scenario. A prescription of the radiative fractions as a function of the oxygen mole fraction in the co-flow could have been made in this case. This option would have guaranteed the correct amount of heat being released due to radiation neglecting, however, any absorption occurring from the combustion products. Nevertheless, even though such an approach would be considered to be a 'safe' option it would not represent a true validation case of the CFD models since a priori knowledge of the radiative fractions for any random fire scenario involving flame extinction is not realistic/possible. Predictive fire modelling, in terms of flame extinction, in reality will be strongly coupled to radiation modelling (through accurate prediction of the resulting radiative fractions). The current study is considered to be an attempt towards this direction by identifying important aspects in fire modelling that should be improved in the future. Additionally, the use of the simpler gray-gas model might lead to over-prediction in the resulting radiative fractions [6] unless a calibration constant is introduced which also puts some limitations in the application of the model to any random scenario. The accuracy of the WSGGM with a dynamically determined beam length in this scenario was satisfactory in terms of predicting the resulting radiative fractions. However, application of the model in more scenarios involving different fuels is needed before making firm statements regarding its accuracy. More specifically, consideration of soot radiation will be essential in scenarios involving heavier hydrocarbon fuels and coupling with WSGGM will be needed. In addition, the use of a dynamically determined beam length will be more challenging when it comes to scenarios involving flame spread where a distinct flame shape cannot be so easily determined.

5.3.3. Model parameter sensitivity

A sensitivity study on the main parameters involved in the flame extinction and re-ignition modelling and the sub-model employed for absorption in the radiation modelling is presented in Figures 11-12 in order to examine their influence on the predictions. Results only on the finest grid size considered in the paper, i.e., 6.25 mm are presented. Two cases where the influence of the re-ignition temperature is examined are presented ($T_{ign} = 1000$ K for EDM and $T_{ign} = 1200$ K for EDC). A case involving EDM with $T_{ign} = 1100$ K and a fixed path length of $L = 7$ cm is shown. Finally a case employing EDM with $T_{ign} = 1100$ K and the gray gas model for radiation, previously described in [16], is presented. The last two cases aim at demonstrating the

25

effect of radiation modelling in terms of predicted combustion efficiencies and radiative fractions.

The choice of the re-ignition temperature, T_{ign}, has a significant influence on the combustion efficiency particularly when the oxygen mole fraction in the oxidizer stream is approaching the extinction limit (i.e., where $X_{O2} \approx 0.12$). Higher or lower T_{ign} values shift the decay phase for the combustion efficiency right or left, respectively, regardless of the employed combustion model. The relative differences observed are of course combustion model dependent given the differences in the resulting flames temperatures obtained with the two models, as previously discussed. The numerical simulation performed with a fixed beam length of 7 cm (calculated for $X_{O2} = 0.21$ in the oxidizer stream considering a rectangular shape for the flame and the experimentally reported flame height of 50 cm) did not reveal a significant influence on the predictions of the combustion efficiencies and the resulting radiative fractions. This finding is perhaps not very surprising since there is a sharp decrease in the combustion efficiency (and the resulting flame volume that would influence L) only when the oxygen mole fraction at the co-flow is close to the extinction limit for CH_4. Nevertheless, a reasonable choice for the beam length, L, is still needed. Values an order of magnitude higher or lower will potentially influence the absorption coefficient, hence, the resulting temperatures and radiative fractions. The final case involving the application of the gray gas model severely over-predicts the resulting radiative fractions, in line with what has been reported in literature in the past [6], and poses some limitations in the application of the model, at least in its current form. Further investigation whether a 'universal' calibration constant in the gray gas model, applicable for a wide range of fuels, could be employed without the need of re-calibration of the constant before every new scenario might be worth exploring in the future.

A sensitivity study (not shown here) on the region above the burner where no extinction is allowed to take place, in order not to influence the primary ignition source, did not reveal any significant influence on the finer grid size cases (i.e., 12.5 mm and 6.25 mm). There was, however, an influence for the 25 mm case given the coarseness of the mesh and the fact that the highest reaction rates are obtained right above the burner in these cases. Doubling the height of this region where no extinction is allowed (from 25 mm to 50 mm) resulted in significantly better predictions for the combustion efficiency in the case of EDM for example. Even though not relevant in simulations with a relatively fine grid size, it is important to the remember that the size
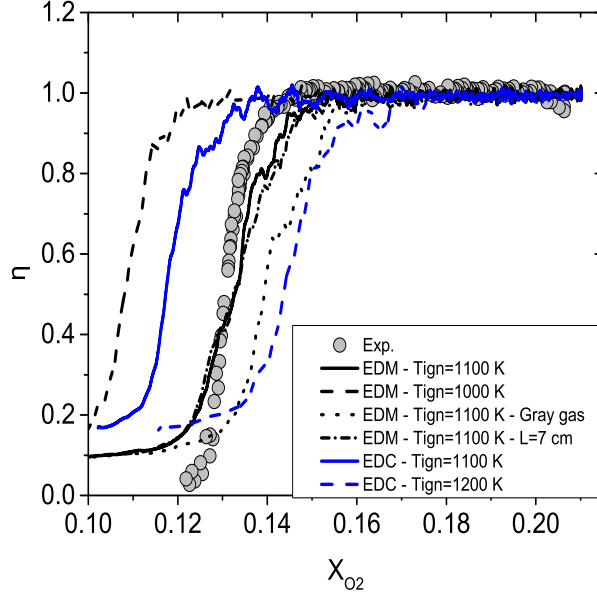
Figure 11: Influence of several model parameters on the predicted combustion efficiency, η, for a grid size of 6.25 mm.

of this region will have an influence in coarse grid calculations.

From the results presented in Figures 11-12, it is observed that the flame extinction performance depends on the T_{ign} value chosen in the numerical simulations. Similar findings were also reported in [6, 4]. More specifically, the specified re-ignition temperature mainly affects the time where extinction occurs with increasing influence as the grid size increases. This is to be expected since the grid size influences the predicted resolve temperatures which directly enter the enthalpy balance and the re-ignition criterion as well. In fact, the influence of the re-ignition model in this case is similar to the one of the flame extinction model revealing the need for accurate modelling of both phenomena. The combined modelling of turbulence, combustion, radiation (also soot modelling when applicable) and flame extinction/re-ignition modelling have a direct influence in the predicted temperatures, hence, also in the evaluation of the enthalpy balance. Dissipative turbulence models could result in a more laminar-like flames, simplified combustion models based on infinitely fast chemistry might not accurately predict CO_2, H_2O and minor species and over/under predictions of the radiative fractions depending on the radiation modelling approach will directly influence the resulting flame
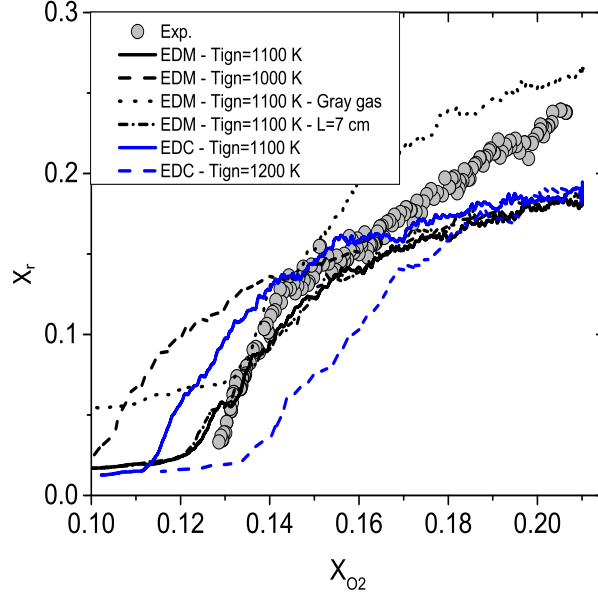
Figure 12: Influence of several model parameters on the predicted radiative fractions, χ_r, for a grid size of 6.25 mm.

temperatures. Adding the need to have accurate predictions over a wide range of grid sizes poses an additional requirement for CFD codes and the employed models. In fact, some of the above findings pose some limitations in the application of the employed approach for modelling flame extinction in scenarios where coarse grids are employed (e.g., due to insufficient computational resources).

6. Conclusions

Large eddy simulations of flame extinction with N_2 as extinguishing agent were presented and the results were compared to the turbulent CH_4 line burner experiments by White et al. (2015). Use of advanced modelling approaches related to turbulence, combustion and radiation was made along with the application of an enthalpy-based extinction model with a locally varying critical flame temperature. The predictive capabilities of the models was analyzed by comparing the numerical predictions for different grid sizes to the experimental thermocouple temperatures, combustion efficiencies and radiative fractions.

The numerical predictions were, overall, in good agreement with the experimental data when fine grid sizes were employed (i.e., 6.25 mm). More specifically, the resulting maximum flame temperatures and flame widths matched reasonably well the experimental profiles at two different heights examined. The numerical simulations were also able to reproduce the decreasing trend of the combustion efficiencies and radiative fractions and the increasing trend in the flame heights, with some discrepancies, when the extinction limit was reached. The influence of the combustion model was found to be significant due to the differences in the resulting flame temperatures which are input in the enthalpy-based flame extinction model. Re-ignition modelling was also important with the choice of the constant re-ignition temperature being equally important as the flame extinction model itself.

Modelling of flame extinction with infinitely fast chemistry using an enthalpy-based extinction model based on the concept of a critical flame temperature can be influenced by many aspects some of which were illustrated in this work. Accurate modelling of combustion (i.e., in terms of resulting mean and rms flame temperatures) and radiation (i.e., in terms of predicted radiative fractions), along with relatively small grid sizes, is a pre-requisite for accurately predicting flame extinction. The choice of a simple re-ignition model based on a constant re-ignition temperature might be worth revisiting in the future by employing a more advanced re-ignition model based on e.g., the local composition and strain rate.

Acknowledgments

References

References

[1] V. Lecoustre, P. Narayanan, H.R. Baum, A. Trouvé, Local extinction of diffusion flames in fires, Fire Safety Science 10 (2011) 583-595.

[2] Z. Hu, Y. Utiskul, J.G. Quintiere, A. Trouvé, Towards large eddy simulations of flame extinction and carbon monoxide emission in compartment fires, Proc. Combust. Inst. 31 (2007) 2537–2545.

[3] J. Vaari, J. Floyd, R. McDermott, CFD Simulations on Extinction of Co-Flow Diffusion Flames, Fire Safety Science 10 (2011) 781-793.

[4] J.P. White, S. Vilfayeau, A.W. Marshall, A. Trouvé, R.J. McDermott, Modeling flame extinction and reignition in large eddy simulations with fast chemistry, Fire Saf. J., 90 (2017) 72-85.

[5] P. Narayanan, H.R. Baum, A. Trouvé, Effect of soot addition on extinction limits of luminous laminar counterflow diffusion flames, Proc. Combust. Inst. 33 (2011) 2539–2546.

[6] S. Vilfayeau, PhD dissertation, University of Maryland, USA, 2015.

[7] S. Vilfayeau, N. Ren, Y. Wang, A. Trouvé, Numerical simulation of under ventilated liquid-fueled compartment fires with flame extinction and thermally-driven fuel evaporation, Proc. Combust. Inst. 35 (3) (2015) 2563–2571.

[8] S. Vilfayeau, J.P. White, P.B. Sunderland, A.W. Marshall, A. Trouvé, Large eddy simulation of flame extinction in a turbulent line fire exposed to air-nitrogen coflow, Fire Saf. J. 86 (2016) 16–31.

[9] A.Y. Snegirev, A.S. Tsoy, Treatment of local extinction in cfd fire modeling, Proc. Combust. Inst. 35 (2015) 2519–2526.

[10] A.Y. Snegirev, Perfectly stirred reactor model to evaluate extinction of diffusion flame, Combust. Flame 162 (2015) 3622–3631.

[11] S.B. Dorofeev, Thermal quenching of mixed eddies in non-premixed flames, Proc. Combust. Inst. 36 (2017) 2947-2954.

[12] G. Maragkos, T. Beji, B. Merci, Advances in modelling in CFD simulations of turbulent gaseous pool fires, Combust. Flame 181 (2017) 22-38.

[13] G. Maragkos, T. Beji, B. Merci, Towards predictive simulations of gaseous pool fires, Proc. Combust. Inst. (2018) - In Press.

[14] J.P. White, E.D. Link, A.C. Trouvé, P.B. Sunderland, A.W. Marshall, J.A. Sheffel, M.L. Corn, M.B. Colket, M. Chaos, H.-Z Yu., Radiative emissions measurements from a buoyant, turbulent line flame under oxidizer-dilution quenching conditions, Fire Saf. J. 76 (2015) 74-84.

[15] V. Sankaran, H. Jiang, M. Colket, S. Zhang, M. Corn, Flame Extinction Model for Fire Suppression Simulations, 9th U.S. National Combustion Meeting, Cincinnati, Ohio, May 17-20, 2015.

[16] G. Maragkos, B. Merci, Large eddy simulations of CH_4 fire plumes, Flow Turb. Combust. 99 (2017) 239-278.

[17] P. Moin, K. Squires, W.H. Cabot, S. Lee, A dynamic subgrid-scale model for compressible turbulence and scalar transport, Phys. Fluids A 3 (1991) 2746-2757.

[18] M.P. Martin, U. Piomelli, G.V. Candler, Sub-grid-Scale Models for Compressible Large-Eddy Simulations, Theoret. Comput. Fluid Dynamics 13 (2000) 361-376.

[19] B.F. Magnussen, On the Structure of Turbulence and a Generalized Eddy Dissipation Concept for Chemical Reaction in Turbulent Flow, 19th AIAA Aerospace Science Meeting, 1981.

[20] B.F. Magnussen, B.H. Hjertager, On mathematical models of turbulent combustion with special emphasis on soot formation and combustion, Proc. Combust. Inst. 16 (1976) 719-729.

[21] Z. Chen, J. Wen, B. Xu, S. Dembele, Large eddy simulation of a medium-scale methanol pool fire using the extended eddy dissipation concept, Int. J. Heat Mass Transf. 70 (2014) 389-408.

[22] I.R. Gran, B.F. Magnussen, A numerical study of a bluff-body stabilized diffusion flame. Part 2. Influence of combustion modeling and finite-rate chemistry, Combust. Sci. Technol. 119 (1996) 191–217.

[23] I.S. Ertesvåg, B.F. Magnussen, The Eddy Dissipation Turbulence Energy Cascade Model, Combust. Sci. Technol. 159 (2000) 213-235.

[24] L.J. Dorigon, G. Duciak, R. Brittes, F. Cassol, M. Galarca, F.H.R. Franca, WSGG correlations based on HITEMP2010 for computation of thermal radiation in non-isothermal, non-homogeneous H2O/CO2 mixtures, Int. J. Heat Mass Transf. 64 (2013) 863-873.

[25] K. McGrattan, S. Hostikka, R. McDermott, J. Floyd, C. Weinschenk, K. Overholt, Fire Dynamics Simulator Technical Reference Guide Volume 1: Mathematical Model, 6th ed., NIST, 2016.

[26] K. McGrattan, S. Hostikka, R. McDermott, J. Floyd, M. Vanella, C. Weinschenk, K. Overholt, Fire Dynamics Simulator User's Guide, NIST Special Publication 1019, Sixth Edition, 2017.

[27] W.M. Pitts, J.C. Yang, R.A. Bryant, L.G. Blevins, M.L. Huber, Characteristics and Identification of Super-Effective Thermal Fire-Extinguishing Agents: Final Report, NGP Project 4C/1/890, NIST Technical Note 1440, 2006.

[28] C.G. Fotache, T.G. Kreutz, C.K. Law, Ignition of Counterflowing Methane versus Heat Air under reduced and Elevated Pressures, Combust. Flame 108 (1997) 442-470.

[29] J.C. Hewson, A.R. Kerstein, Local extinction and reignition in non-premixed turbulent CO/H2/N2 jet flames, Combust. Sci. Technol. 174 (2002) 35-66.

[30] K. McGrattan, S. Hostikka, R. McDermott, J. Floyd, M. Vanella, C. Weinschenk, K. Overholt, Fire Dynamics Simulator Technical Reference Guide Volume 3: Validation, NIST Special Publication 1018-3, Sixth Edition, 2018.

[31] P. Chatterjee, Y. Wang, K.V. Meredith, S.B. Dorofeev, Application of a subgrid soot-radiation model in the numerical simulation of a heptane pool fire, Proc. Combust. Inst. 35 (2015) 2573-2580.

[32] N. Ren, Y. Wang, S. Vilfayeau, A. Trouvé, Large eddy simulation of turbulent vertical wall fires supplied with gaseous fuel through porous burners, Combust. Flame 169 (2016) 194-208.

[33] B. Lilleberg, D. Christ, I.S. Ertesvåg, K.E. Rian, R. Kneer, Numerical Simulation with an Extinction Database for Use with the Eddy Dissipation Concept for Turbulent Combustion, Flow Turb. Combust. 91 (2013) 319-346.

[34] M.T. Lewandowski, I.S. Ertesvåg, Analysis of the Eddy Dissipation Concept formulation for MILD combustion modeling, Fuel 224 (2018) 687-700.

[35] L. Kjäldman, A. Brink, M. Hupa, Micro Mixing Time in the Eddy Dissipation Concept, Combust. Sci. Technol. 154 (2000) 207-227.

[36] A. Brown, M. Bruns, M. Gollner, J. Hewson, G. Maragkos, A. Marshall, R. McDermott, B. Merci, T. Rogaume, S. Stoliarov, J. Torero, A. Trouvé, Y. Wang, E. Weckman, Proceedings of the first workshop organized by the IAFSS Working Group on Measurement and Computation of Fire Phenomena (MaCFP), Fire Saf. J. 101 (2018) 1-17.

[37] S.B. Pope, Ten questions concerning the large-eddy simulation of turbulent flows, New Journal of Physics 6 (2004) 1-24.

[38] I. Celik, M. Klein, J. Janicka, Assessment Measures for Engineering LES Applications, J. Fluids Eng. 131 (2009) 031102.

[39] V.M. Le, A. Marchand, S. Verma, R. Xu, J. White, A.W. Marshall, T. Rogaume, F. Richard, J. Luche, A. Trouvé, Simulations of a Turbulent Line Fire with a Steady Flamelet Combustion Model and Non-Gray Gas Radiation Models, Submitted for publication in Fire Safety Journal (2018).

[40] G. Cox, On Radiant Heat Transfer from Turbulent Flames, Combust. Sci. Technol. 17 (1977) 75–78.